J Neurophysiol 100: 1255–1264, 2008.
First published July 16, 2008; doi:10.1152/jn.90715.2008.

Short-Term Synaptic Depression and Recovery at the Mature Mammalian Endbulb of Held Synapse in Mice

Yong Wang and Paul B. Manis
Department of Otolaryngology/Head and Neck Surgery, University of North Carolina, Chapel Hill, North Carolina

Submitted 25 June 2008; accepted in final form 15 July 2008

Wang Y, Manis PB. Short-term synaptic depression and recovery at the mature mammalian endbulb of Held synapse in mice. *J Neurophysiol* 100: 1255–1264, 2008. First published July 16, 2008; doi:10.1152/jn.90715.2008. The endbulb of Held synapses between the auditory nerve fibers (ANF) and cochlear nucleus bushy neurons convey fine temporal information embedded in the incoming acoustic signal. The dynamics of synaptic depression and recovery is a key in regulating synaptic transmission at the endbulb synapse. We studied short-term synaptic depression and recovery in mature (P22-38) CBA mice with stimulation rates that were comparable to sound-driven activities recorded in vivo. Synaptic depression in mature mice is less severe (~40% at 100 Hz) than reported for immature animals and the depression is predominately due to depletion of releasable vesicles. Recovery from depression depends on the rate of activity and accumulation of intracellular Ca^{2+} at the presynaptic terminal. With a regular stimulus train at 100 Hz in 2 mM external [Ca^{2+}], the recovery from depletion was slow (τ_{slow}, ~2 s). In contrast, a fast (τ_{fast}, ~25 ms), Ca^{2+}-dependent recovery followed by a slower recovery (τ_{slow}, ~2 s) was seen when stimulus rates or external [Ca^{2+}] increased. In normal [Ca^{2+}], recovery from a 100-Hz Poisson-like train is rapid, suggesting that Poisson-like trains produce a higher internal [Ca^{2+}] than regular trains. Moreover, the fast recovery was slowed by approximately twofold in the presence of calmidazolium, a Ca^{2+}/calmodulin inhibitor. Our results suggest that endbulb synapses from high spontaneous firing rate auditory nerve fibers normally operate in a depressed state. The accelerated synaptic recovery during high rates of activity is likely to ensure that reliable synaptic transmission can be achieved at the endbulb synapse.

INTRODUCTION

Bushy cells in the mammalian anteroventral cochlear nucleus (AVCN) receive obligatory synaptic input from the auditory nerve fibers (ANFs). The bushy cells are highly specialized to encode fine temporal information embedded in the acoustic signal conveyed by the auditory nerve fibers (Manis 2008; Trussell 2008). Historically, synaptic transmission at the endbulb terminal was believed to be extremely secure, and a one-to-one ratio of pre- and postsynaptic spikes was suggested (Pfeiffer 1966). However, despite the presence of a primary-like peristimulus spike-time histogram to tone bursts in vivo, the spike patterns of a bushy cell may not faithfully reflect the presynaptic activity of a given ANF (Kopp-Scheinpflug et al. 2002) due to several factors. These include the convergence of ANFs onto bushy neurons (Leao et al. 2005; Liberman 1991; Nicol and Walmsley 2002; Rothman et al. 1993; Ryugo and Parks 2003; Xu-Friedman and Regehr 2005a,b), the effects of inhibition from the dorsal cochlear nucleus (DCN) and superior olivary complex (Caspary et al. 1994; Wickesberg and Oertel 1988), activity-dependent modulation of presynaptic release probability (Brenowitz and Trussell 2001a; Turecek and Trussell 2001), and synaptic depression during high rates of activity (Oleskevich et al. 2000; Wang and Manis 2006; Xu-Friedman and Regehr 2005b; Yang and Xu-Friedman 2008; Zhang and Trussell 1994). More recently, recordings from presumed AVCN spherical bushy cells in vivo have suggested that as many as 50% of ANF spikes may fail to drive bushy cells (Kopp-Scheinpflug et al. 2002, 2003). In vitro recordings have also revealed that the response entrainment of bushy cells to ANF stimulation falls <50% when trains of shock stimuli are delivered at ≥200 Hz at room temperature (Wang and Manis 2006; Xu-Friedman and Regehr 2005b). The spontaneous firing rates of single ANFs in normal hearing mice of the CBA strain can exceed 100 spike/s, and ANFs can have sustained sound-driven discharge rates of 200–350 Hz (Taberner and Liberman 2005). Similar discharge rates have been reported in cats (Liberman 1978; Sachs and Abbas 1974), guinea pigs (Winter et al. 1990), and gerbils (Ohlemiller et al. 1991). Thus synaptic depression during high rates of ANF activity, and subsequent recovery during periods of lower activity, can significantly shape the functional relationship between the ANF and bushy cell.

To characterize the dynamic changes in synaptic efficacy at the endbulb synaptic terminal, we studied the time course of synaptic depression and recovery with high-frequency stimulation. We used both regularly spaced and stimuli with exponentially distributed interval distributions (Poisson-like), similar to the spontaneous firing of auditory nerve fibers, to shock small populations of auditory nerve fibers in a cochlear nucleus slice preparation. We varied external bath Ca^{2+} concentration and stimulus rates to examine the effect of intracellular Ca^{2+} accumulation on synaptic recovery from short-term depression. We also investigated the presumptive role of AMPA receptor desensitization in synaptic depression using a low-affinity AMPA receptor antagonist, γ-D-glutamylglycine (γ-DGG), and we examined the role of Ca^{2+}/calmodulin signaling in regulating recovery from depression. Our results suggest that synaptic depression due to vesicle depletion, as opposed to receptor desensitization, shapes the responses of bushy cells when challenged by high firing rates in auditory nerve fibers in mature mice, and that a fast, calcium-dependent recovery process may help minimize the effects of depression following bursts of activity at high rates.

Present address and address for reprint requests and other correspondence: Y. Wang, University of Utah, Otolaryngology/Head and Neck Surgery, 30 N 1900 E, Salt Lake City, UT 84132 (E-mail: yong.wang@hsc.utah.edu).

The costs of publication of this article were defrayed in part by the payment of page charges. The article must therefore be hereby marked "*advertisement*" in accordance with 18 U.S.C. Section 1734 solely to indicate this fact.

METHODS

Animal subjects

CBA/Caj mice (Jackson Lab, Bar Harbor, ME) from an in-house colony, 22–38 days old, were used for all electrophysiological recordings. No developmental changes in synaptic properties have been found in animals of this age range (Wang and Manis 2005). All experiments were done in accordance with protocols approved by the Institutional Animal Care and Use Committee at the University of North Carolina at Chapel Hill.

Cochlear nuclear slice preparation

Mice were anesthetized with ketamine (100 mg/kg)/xylazine (10 mg/kg ip), and then decapitated once they were areflexic to paw pinches. The brain stem including the cochlear nucleus was immediately dissected out and immersed in prewarmed (34°C) dissecting artificial cerebrospinal fluid (ACSF), which differed from recording ACSF by containing high Mg^{2+} (3.8 mM) and low Ca^{2+} (0.2 mM). The standard recording ACSF contained (in mM) 130 NaCl, 3 KCl, 1.25 KH_2PO_4, 10 glucose, 20 $NaHCO_3$, 2 $CaCl_2$, and 2 $MgSO_4$ and was bubbled with 95% O_2-5% CO_2 to a pH of 7.4. Brain stems were trimmed, mounted on a cutting block, and 200–250 μm parasagittal sections of the cochlear nucleus were sliced on an oscillating tissue slicer (Vibratome 1000, Technical Products, St. Louis, MO). After incubation for ~30 min at 34°C in recording ACSF, each slice was secured in the recording chamber while ACSF flowed through at a rate of 3–5 ml/min. To study receptor desensitization, 2 mM γ-DGG was included in the recording ACSF. All recordings were made at 34°C heated with a dual inline and chamber heater (Warner Instruments, Hamden, CT).

Electrophysiological recordings

Cells were visualized with an upright Zeiss Axioskop FS2 Plus (Zeiss, Germany) equipped with a water-immersion lens (×40) and differential interference contrast optics. To enhance image contrast in slices from older animals, the field diaphragm was closed nearly all the way without using the infrared filter, and the condenser was aligned slightly eccentrically (Kachar 1985). Patch electrode pipettes were pulled from borosilicate glass (KG-33, Garner Glass, Claremont, CA) with a Sutter P2000 puller (Sutter Instruments, San Francisco, CA), and have a typical resistance of 3–8 MΩ. Tips of recording pipettes were coated with silicone elastomer (Sylgard 184, Dow Corning, Midland, MI) before use. For evoked excitatory postsynaptic current (EPSC) recordings, a Cs^+-based electrode solution containing 2–5 mM QX314 (Tocris Cookson, Bristol, UK) was used to minimize contamination from potassium and sodium conductances. The solution contained (in mM) 125 $CsMeSO_3$, 15 CsCl, 5 EGTA, 10 HEPES, 4 MgATP, 10 creatine phosphate, and 0.3 GTP and was adjusted to pH 7.2 with CsOH. Whole cell recordings were made with an Axopatch 200B amplifier (Molecular Devices, Foster City, CA) under the control of in-house software written in MATLAB. Whole cell access resistance was routinely <15 MΩ and compensated to a typical value of ~75% on-line with a 20-μs lag time.

For auditory nerve evoked responses, a 75-μm diameter concentric stimulating electrode was placed on the auditory nerve root. A stimulus-response function was measured and used to determine the EPSC threshold. The stimulus strength was then adjusted to be 1.5 times the threshold necessary to elicit reliable EPSCs. To be accepted for analysis, the EPSC elicited by the lowest-intensity stimulus had to be all-or-none and ≥1 nA in amplitude as expected for a large endbulb of Held synapse on to bushy cells (Isaacson and Walmsley 1996; Wang and Manis 2005).

To test synaptic depression and recovery, we recorded evoked postsynaptic currents in voltage clamp in response to trains of 15–20 shocks to the auditory nerve. Shock trains at 100, 200, and 300 Hz were delivered every 10 s. At the end of each shock train, a test pulse with variable delay was presented to measure the synaptic recovery from depression. For a given test pulse latency, five trials were repeated, and the responses were averaged. However, as opposed to regular trains, auditory nerve fibers fire with interspike intervals that are exponentially distributed with a dead time (Li and Young 1993; Rodieck et al. 1962). These exponentially distributed (or "Poisson with dead time") sequences were generated by randomly choosing intervals from a random exponential distribution with the prescribed mean rate. Intervals shorter than a dead time of 0.7 ms were excluded to account for the absolute refractory period of ANFs. To test depression and recovery with Poisson-distributed spike trains, five independent sequences with mean rates of 100 and 200 Hz, 500 ms long, were generated. Recovery test pulses were delivered at different intervals at the end of Poisson-like stimulus trains as in the preceding text. Each recovery time point was tested five times with a different Poisson-like train each time, and the responses were averaged. Only one recovery interval was tested following each stimulus sequence. For comparison with Poisson-like stimulus trains, regular shock trains at 100 and 200 Hz with 500-ms duration were also used to test depression and recovery.

Data analysis

Evoked EPSC amplitudes were measured from the current baseline to the peak of the event. EPSC amplitudes were then normalized to the average amplitude of the first EPSC in the train. Peak amplitude time courses were fitted with a single-exponential function. The recovery responses were also normalized to the average amplitude of the first EPSC in the train and were fitted against a single- or double-exponential function.

Statistical analysis (*t*-test or ANOVA) and curve fits were performed with Prism 4.0 (San Diego, CA). Significance was determined for an α value of <0.05. Data are presented as means ± SE.

RESULTS

Activity-dependent synaptic depression

Endbulb terminals onto AVCN bushy neurons show high release probability when activated from a quiescent state (Oleskevich and Walmsley 2002; Wang and Manis 2005). With repeated stimulation, synaptic responses at the endbulb of Held terminal show significant rate-dependent depression (Fig. 1*B*). In endbulb terminals of young mouse (Oleskevich et al. 2004; Yang and Xu-Friedman 2008), their analogous terminals in chick nucleus magnocellularis (NM) (Brenowitz and Trussell 2001a) or calyx terminals in medial nucleus of the trapezoid body (MNTB) of young mice (Joshi and Wang 2002), synaptic depression reaches ~90% at 100 Hz. In contrast, we found that, in mature CBA mice (p22-38), the synaptic response depressed by 36.7 ± 3.7% (n = 10) at the end of 15–20 stimuli at 100 Hz, whereas the responses to 200- and 300-Hz shocks were depressed by 51.5 ± 3.9% (n = 9), and 68.2 ± 3.0% (n = 7), respectively, in 2 mM external [Ca^{2+}]. While receptor desensitization may contribute to the initial phase of the fast depression during high-frequency stimulus trains (Yang and Xu-Friedman 2008), we found that short term synaptic depression can be well described with a single-exponential function (Fig. 1*B*) when the stimulation train duration is limited to 100–200 ms. The time constants of depression at 100, 200, and 300 Hz were 49.2 ± 3.6, 33.3 ± 2.1, and 17.2 ± 1.2 ms, respectively. We also found that the endbulb synapse exhibited a second, slow depression of 15–20% when stimulation trains were prolonged to 500 ms (see following text)

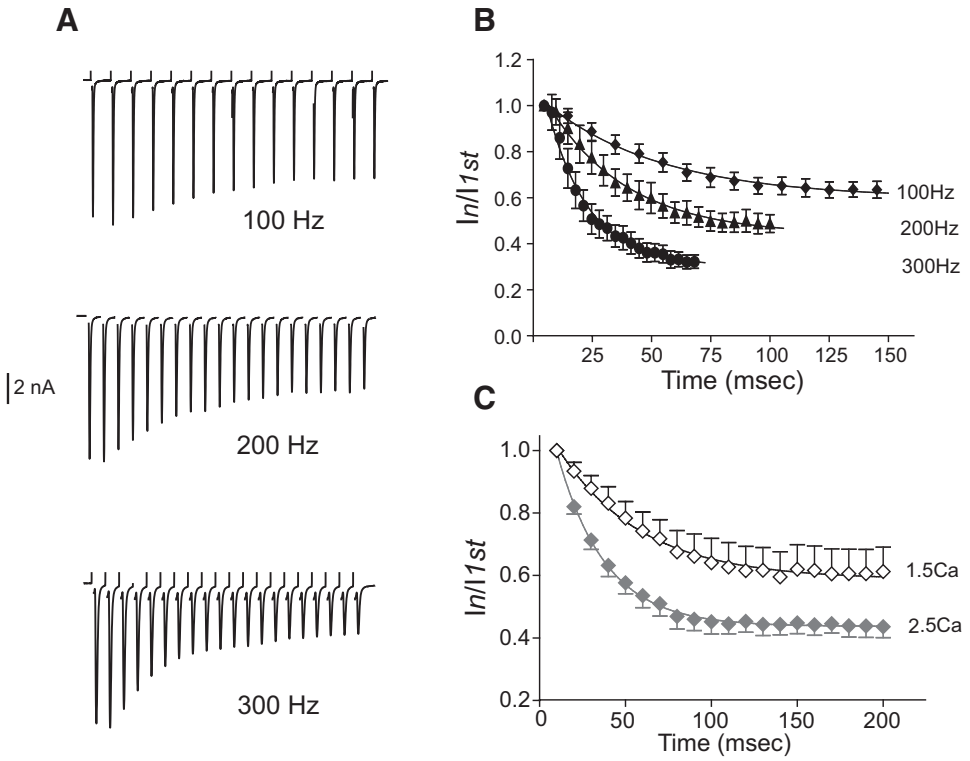

FIG. 1. Activity rate and external $[Ca^{2+}]$ dependent synaptic depression. *A*: examples of a bushy neuron excitatory postsynaptic current (EPSC) response to trains of auditory nerve fiber stimulation at different rates. Traces are averages of 40 trials for each frequency; stimulus artifacts have been erased. *B*: evoked EPSCs normalized to the amplitude of the 1st EPSC at 100-, 200-, and 300-Hz shock stimulation in 2 mM external $[Ca^{2+}]$. Superimposed lines are single-exponential fits of the data. *C*: normalized EPSC responses to 100-Hz stimulus trains at 1.5 and 2.5 mM external $[Ca^{2+}]$.

(also see Wong et al. 2003). We did not study the slow depression further. Varying external $[Ca^{2+}]$ changed the rate of synaptic depression (Fig. 1*C*). Synaptic depression induced by trains of 20 pulses delivered at 100 Hz was 38.8 ± 7.9% in 1.5 mM $[Ca^{2+}]$ and 56.4 ± 3.4% in 2.5 mM $[Ca^{2+}]$ ($n = 7$), respectively. When normalized, the time course of synaptic depression at the two different Ca^{2+} concentrations differed by nearly a factor of two ($\tau_{dep} = 48.1 \pm 2.8$ ms for 1.5 mM $[Ca^{2+}]$ vs. 27.9 ± 0.6 ms for 2.5 mM $[Ca^{2+}]$; $P < 0.0001$, ANOVA). These results are consistent with a vesicular depletion and/or receptor desensitization mechanism rather than presynaptic Ca^{2+} channel inactivation, as the primary cause of synaptic depression for rates ≥100 Hz as reported at the calyx terminal in MNTB (Forsythe et al. 1998; Xu and Wu 2005). These results do not, however, exclude the possibility that a transient decrease in Ca^{2+}-triggered release probability also contributes to short-term synaptic depression (Bellingham and Walmsley 1999; Wu and Borst 1999).

No receptor desensitization in mature endbulb synapse

Synaptic depression at the young mouse endbulb terminal (Yang and Xu-Friedman 2008) as well as in analogous terminals in chick NM (Raman and Trussell 1992) and the MNTB calyx of Held (Wong et al. 2003) has been shown to result, in part, from postsynaptic AMPA receptor desensitization. We thus examined the role of receptor desensitization in synaptic depression during repetitive stimulation at the mature endbulb. Because the endbulb AMPA receptors are not saturated under our recording conditions (Wang and Manis 2005), we used a low-affinity, rapidly dissociating competitive AMPA receptor antagonist γ-D-glutamylglycine (γ-DGG) to investigate the potential role of postsynaptic receptor desensitization in bushy neurons of the AVCN during synaptic depression. γ-DGG has been shown to have fast off-rate constants that can provide optimal relief from desensitization in the range of 90% (Wong et al. 2003). If desensitization played a role in synaptic depression during high rates of stimulation, we would expect that depression should be reduced in the presence of γ-DGG. We found that 2 mM γ-DGG reduced the initial EPSC amplitude by ~70%, from 5.1 ± 0.7 to 1.7 ± 0.5 nA ($n = 5$, $P < 0.01$, paired *t*-test; Fig. 2*A*). However, there was no change in synaptic depression in the presence of γ-DGG. At 100 Hz (Fig. 2*B*), the normalized steady-state depression with and without γ-DGG was 37.7 ± 3.6 and 38.2 ± 5.5% ($n = 4$, $P = 0.49$ paired *t*-test), respectively. γ-DGG did not relieve desensitization even when deeper depression was induced with 200-Hz shock trains (depression was 56.4 ± 3.2 with and 56.7 ± 3.1% without γ-DGG, $n = 4$, $P = 0.97$, paired *t*-test). We also examined the ratio of $EPSC_2/EPSC_1$ at 100- and 200-Hz trains with and without γ-DGG to see if desensitization might occur at the beginning of the train (Yang and Xu-Friedman 2008). We found no difference in the $EPSC_2/EPSC_1$ ratio in the presence of γ-DGG, indicating desensitization does not appear to play a role even early during the stimulus train. The $EPSC_2/EPSC_1$ ratios were 0.94 ± 0.03 (control) and 0.97 ± 0.05 (with γ-DGG, $n = 4$, $P = 0.5$, paired *t*-test) at 100 Hz, whereas the $EPSC_2/EPSC_1$ ratio were 0.94 ± 0.01 (control) and 0.99 ± 0.02 (with γ-DGG, $n = 4$, $P = 0.12$, paired *t*-test) at 200 Hz. Furthermore, examination of the amplitude of miniature spontaneous EPSCs 25 ms immediately following 200-Hz EPSC trains (76.6 ± 10.0 pA), when receptors would presumably still be under the influence of desensitization (Otis et al. 1996; Raman and Trussell 1992), showed no amplitude reduction when compared with the baseline miniature EPSC (mEPSC) amplitude (70.7 ± 5.4 pA, $n = 5$, $P = 0.46$, paired *t*-test, Fig. 2*C*). However, we did notice a significant increase in mEPSC frequency, consistent with elevated presynaptic $[Ca^{2+}]_i$ (see following text). Taken

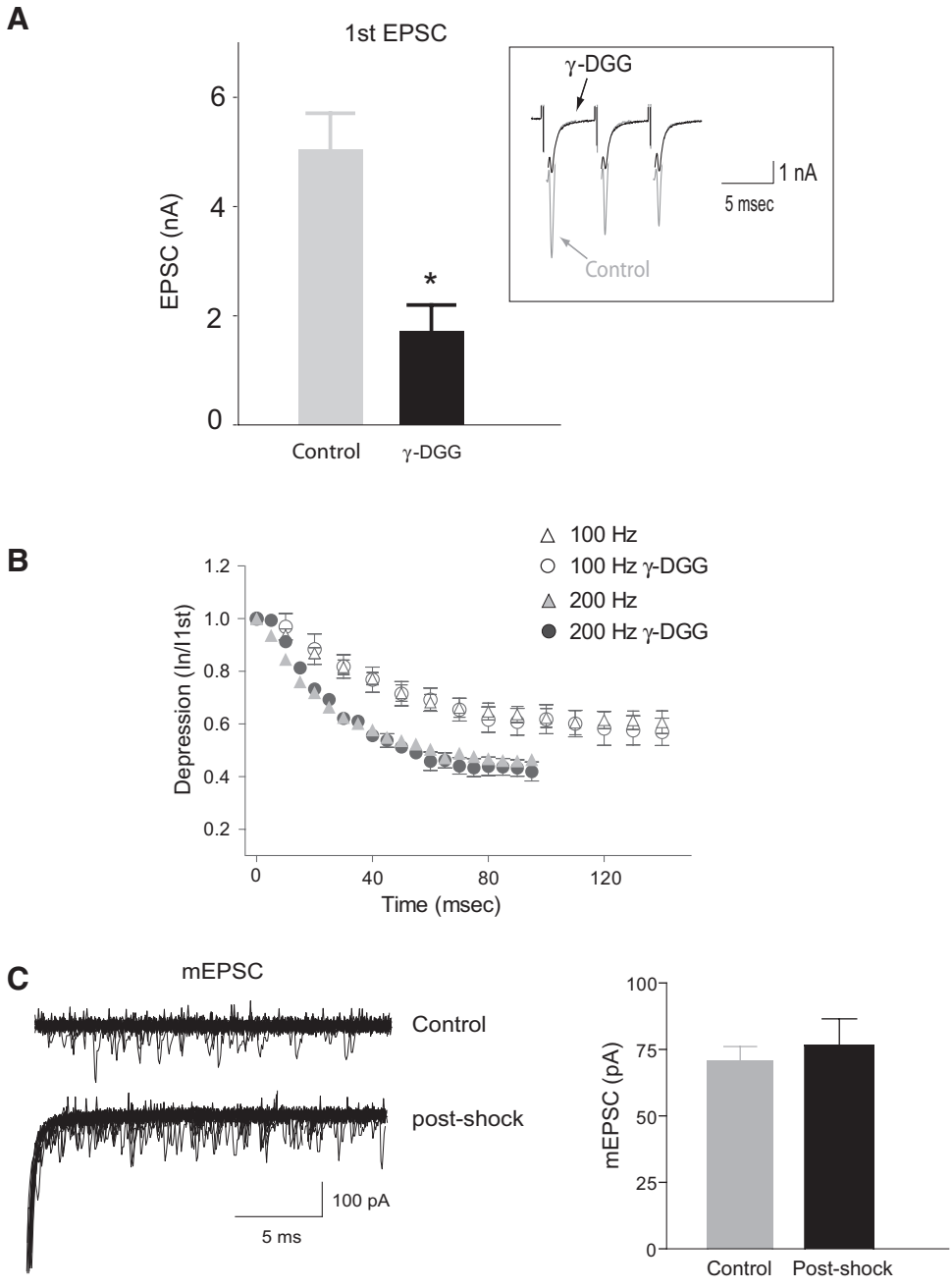

FIG. 2. There is no relief of synaptic depression by 2 mM D-glutamylglycine (γ-DGG). *A*: evoked EPSC response is significantly reduced in the presence of 2 mM low-affinity, competitive AMPA receptor antagonist γ-DGG. *Inset*: sample traces of EPSCs recorded in the presence and absence of γ-DGG from a bushy neuron. *B*: γ-DGG has no effect on the normalized synaptic depression at 100- and 200-Hz stimulus rates. *C*: spontaneous miniature EPSCs before and immediately after 200-Hz shock stimulus trains. Notice the falling phase of EPSCs in postshock traces. Twenty-five individual traces were superimposed.

together, these data suggest that AMPA receptor desensitization does not play a significant role in synaptic depression during train stimulation at the endbulb in mature mice, consistent with data from mature MNTB neurons (Renden et al. 2005). Therefore the strength of synaptic transmission at the endbulb of Held terminal in mature mice, under conditions of normal sensory activation, will depend principally on the relative rates of presynaptic vesicle depletion and recovery from depletion. To further understand the recovery from depletion, we turned to analysis of the time course of recovery following depression.

Single- or two-phased recovery from short-term synaptic depression

We found that recovery from synaptic depression was rate dependent and exhibited two distinct patterns. At 100 Hz in 2 mM $[Ca^{2+}]$, recovery follows a slow time course. In contrast, at higher rates, two recovery phases are evident (Fig. 3), similar to those seen at the endbulb in younger animals (Yang and Xu-Friedman 2008) and in the calyx terminal in MNTB (Sakaba and Neher 2001a; Wang and Kaczmarek 1998; Wu and Borst 1999). In 2 mM $[Ca^{2+}]$, a 100-Hz shock train produced ~40% synaptic depression, and no significant recovery of EPSC amplitude was evident for the first 500 ms after the shocks. In a marked contrast, a very fast recovery phase followed by a slower recovery was observed when stimuli were delivered at 200 and 300 Hz. The recovery time course after 200- and 300-Hz shocks can be fit with a double-exponential function. For 200-Hz stimulus trains, the fast and slow recovery time constants were $\tau_{fast} = 19.9 \pm 4.0$ ms (49.0 ± 4.1% of total recovery) and $\tau_{slow} = 1.73 \pm 0.74$ s ($n = 9$), whereas for

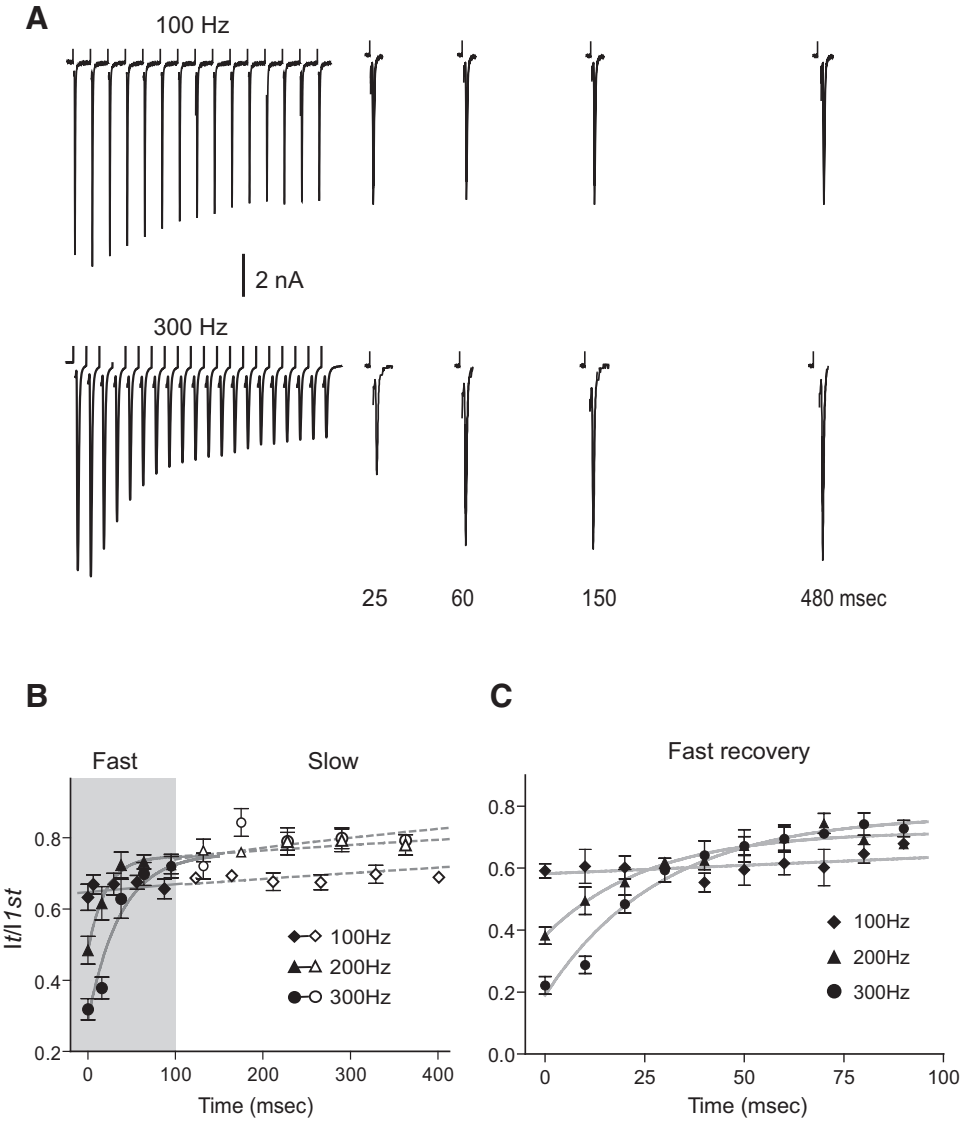

FIG. 3. Recovery from depression depends on presynaptic firing rate. *A*: sample records of recovery from synaptic depression at different intervals after shock stimulus trains. Five trials for each recovery interval were recorded and EPSC responses were averaged. Synaptic depression traces were averaged from 30–40 trails. *B*: recovery from short-term depression after 100, 200, and 300 shock trains. Recovery time courses were fit with a bi-exponential function for 200- and 300-Hz trains, whereas a single-exponential function fit was used for 100-Hz shock trains. — and - - -, the fast and slow phase, respectively, derived from the bi-exponential fits. *C*: in a different set of cells, synaptic recovery was tested at a higher sampling rate within 100 ms immediately after the shock train at 100, 200, and 300 Hz. Data from 200- and 300-Hz recovery were fitted with a single-exponential function. Data from 100 Hz were fitted with a linear regression.

300-Hz shock trains, the recovery time constants were τ_{fast} = 40.6 ± 9.5 ms (66.1 ± 7.0%) and τ_{slow} = 1.50 ± 1.23 s (n = 7). Interestingly, after the initial phase of fast recovery, the overall recovery achieved following the stimulus train at 200 and 300 Hz was significantly greater than that for the 100-Hz train (data pooled for responses tested 100–500 ms following the end of the stimulus train, $P < 0.0001$, t-test). At 100 Hz, no fast recovery was visible, but the slow recovery time constant was 1.99 ± 0.94 s (Fig. 3*B*). At all frequencies, the EPSC amplitudes returned to their initial values within 10 s following the stimulus train. Because our fast recovery time constants at 200 and 300 Hz were very fast (Fig. 3*B*) and did not seem to show a stimulus rate-dependent increase as previously reported (Dittman and Regehr 1996; Sakaba and Neher 2001a; Stevens and Wesseling 1999; Wang and Kaczmarek 1998), we sampled the first 100 ms following the shock train at higher resolution to better explore the fast recovery phase. Figure 3*C* shows results from a different set of cells in which recovery test pulses were given at 10-ms intervals for the first 100 ms after the shock train. The recovery time course can be well fit to a single-exponential function for 200- and 300-Hz shocks but not for the 100-Hz shock stimuli, which is better fit to a straight line with a slope of 0.0005 ± 0.0003/ms, not significantly different from a slope of 0. The fast recovery time constants measured within 100 ms after the shock trains were τ_{fast} = 25.8 ± 6.4 ms and τ_{fast} = 29.1 ± 5.4 ms (n = 4) respectively for 200 and 300 shock trains. Again, the fast recovery at 200 and 300 Hz overshot the recovery level following 100-Hz stimulation, beginning ~50 ms after the end of the stimulus train.

Activity-dependent intracellular Ca^{2+} accumulation and the fast synaptic recovery

Synaptic vesicle release is a process that is dependent on the influx of Ca^{2+} through Ca^{2+} channels at the synaptic terminal (Zucker and Regehr 2002). In calyceal terminals of MNTB, there is a significant accumulation of Ca^{2+} at the presynaptic terminal during high rates of activity (Bollmann et al. 2000; Helmchen et al. 1997; Schneggenburger and Neher 2000). To manipulate the terminal intracellular [Ca^{2+}] during repetitive firing, we altered the shock stimulus rate along with external bath Ca^{2+} concentration. This allowed us to produce different final levels of synaptic depression at a single stimulus fre-

quency or the same level of depression with different stimulus frequencies. In this set of bushy neurons, stimulus trains of 100 Hz produced 38.8 ± 7.9% depression in 1.5 mM Ca^{2+} ($n = 7$), and only a slow recovery was evident ($\tau_{slow} = 3.66 \pm 1.04$ s; Fig. 4). However, with either an elevated Ca^{2+} concentration (2.5 mM) or a higher rate of stimulation (200 Hz), a fast recovery was induced (Fig. 4*B*). With either 2.5 mM Ca^{2+}/100 Hz stimuli or 1.5 mM Ca^{2+}/200 Hz stimuli, nearly identical depression time courses and levels were achieved with final depression of 56.4 ± 3.7% ($\tau_{dep} = 27.7 \pm 0.6$ ms, $n = 7$) and 52.0 ± 6.7% ($\tau_{dep} = 27.0 \pm 1.3$ ms; $n = 6$), respectively (Fig. 4*A*), even though the initial release probability and EPSC amplitude under these two conditions were very different (Fig. 4*A, inset*). We found that synaptic depression recovered with similar time course ($\tau_{fast} = 35.6 \pm 14.5$ ms, $\tau_{slow} = 2.26 \pm 0.21$ s for 1.5 mM Ca^{2+}, 200 Hz vs. $\tau_{fast} = 34.9 \pm 7.7$ ms, $\tau_{slow} = 1.75 \pm 0.11$ s for 2.5 mM Ca^{2+}, 100 Hz). When intracellular $[Ca^{2+}]$ was further elevated in 2.5 mM Ca^{2+} and 200 Hz, the fast recovery constant was $\tau_{fast} = 40.5 \pm 15.7$ ms, whereas the $\tau_{slow} = 2.54 \pm 0.22$ s, and the recovery was more complete than that in 1.5 mM Ca^{2+} and 100 Hz (Fig. 4*B*). Due to the relatively high variability of the EPSC amplitudes during the dynamic period of the fast recovery, the recovery time constant estimates from double-exponential fits have a fairly wide range. Nevertheless taken together with data in 2 mM Ca^{2+}, our results suggest that terminal $[Ca^{2+}]_i$ induced by repetitive firing has to reach a certain critical level to trigger the fast recovery mechanism, and once triggered, the time course of this fast recovery is less dependent on further $[Ca^{2+}]_i$ increases.

Involvement of Ca^{2+}/calmodulin signaling during fast synaptic recovery

The Ca^{2+}/calmodulin signaling pathway has been implicated in multiphasic recovery from depression in MNTB neurons (Sakaba and Neher 2001a). However, our analysis of the fast recovery time course at the unperturbed AVCN endbulb did not suggest more than one rapid recovery component. To test whether Ca^{2+}/calmodulin signaling involved in the fast synaptic recovery at the endbulb synaptic terminal after a train, we bathed the terminals with a membrane permeable pharmacological inhibitor of calmodulin, calmidazolium. Despite previously reported effects of calmidazolium on certain types of Ca^{2+} channels (Kindmark et al. 1994; Nakazawa et al. 1993), we found no effect of calmidazolium on evoked EPSCs (data not shown), suggesting a tight coupling between Ca^{2+} channel and release mechanism at the endbulb terminal similar to the calyx terminal (Fedchyshyn and Wang 2005; Sakaba and Neher 2001a; Wadel et al. 2007). Figure 5 shows that the rapid synaptic recovery in 2 mM Ca^{2+} at 200 Hz was significantly retarded in the presence of 20 μM calmidazolium. The recovery time constant was 47.6 ± 9.0 ms under control conditions (in which the bath included 0.1% DMSO), whereas the τ_{fast} was 116.3 ± 38.3 ms in the presence of calmidazolium ($P = 0.039$, 1-tailed *t*-test, $n = 4,7$; *, *t*-test *P* values <0.05 for recovery level at different time points).

Depression and recovery with Poisson-like spike trains

Spontaneous firing rates (SR) of auditory nerve fibers recorded from CBA mice can exceed 100 spike/s (Taberner and Liberman 2005). Spontaneous activity in the auditory nerve follows a Poisson-like interspike interval distribution with a refractory period or "dead time." If the kinetics of transmitter release are nonlinear, then occasional periods of high-frequency firing within a Poisson train may cause transient high intracellular Ca^{2+} accumulation. Consequently, the magnitude of depression and the recovery kinetics might differ depending on the specific pattern of stimulation. We presented stimuli that mimicked in vivo spike trains with Poisson-distributed interspike intervals (see METHODS). We compared these Poisson-distributed trains with regular trains, at average rates of 100 and 200 Hz for 500 ms and measured depression during the stimulus train and recovery immediately after the train. Due to the relatively large fluctuation of EPSC amplitudes in Poisson-like trains (also see Hermann et al. 2007), we averaged the last three EPSCs at the end of a 500-ms train to represent the mean depression at the end of the train. Figure 6*A* shows the typical time course of synaptic depression of a cell for both a regular and Poisson-like 100-Hz train. Synaptic depression was significantly different at 200 Hz but not at 100 Hz between regular trains and Poisson-like trains of the same rate (Fig. 6*B*). The final levels were 37.2 ± 2.5% (regular) and 40.4 ± 2.5%

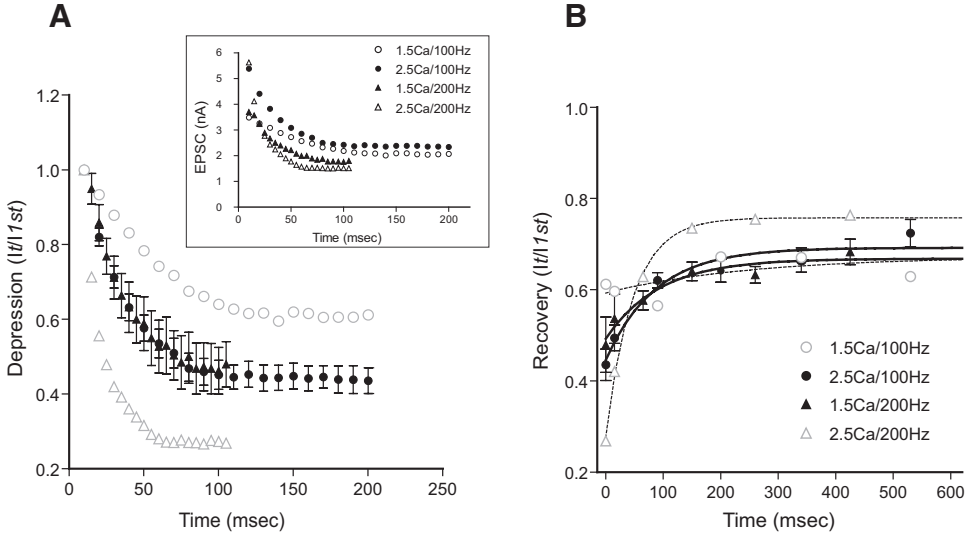

FIG. 4. $[Ca^{2+}]_i$ dependence of rapid synaptic recovery. *A*: normalized synaptic depression under combinations of low (1.5 mM) or high (2.5 mM) external $[Ca^{2+}]$ and low (100 Hz) or high (200 Hz) stimulus rate. Error bars were omitted for 1.5 mM Ca^{2+}/100-Hz and 2.5 mM Ca^{2+}/200-Hz conditions in both *A* and *B* for clarity. Symbol legends in *B* apply to *A*. *Inset*: amplitudes of EPSC trains from varying external $[Ca^{2+}]$ and stimulus rates. *B*: recovery from synaptic depression under various combinations of external $[Ca^{2+}]$ and stimulus rates.

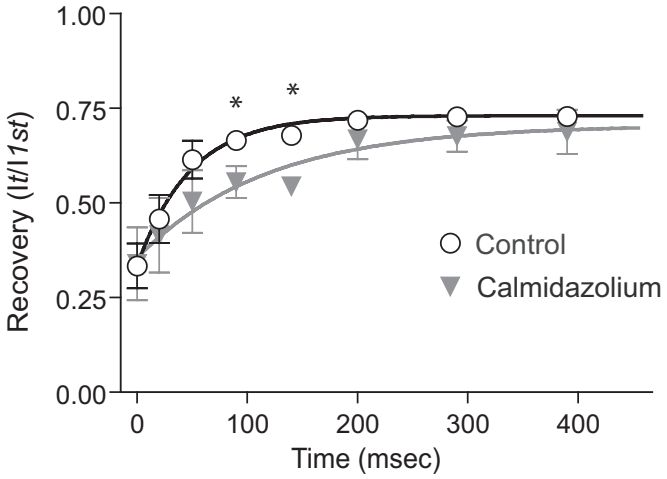

FIG. 5. Effect of calmidazolium on rapid synaptic recovery. Group data of synaptic recovery from 200-Hz stimulus trains in the presence ($n = 4$) and absence ($n = 7$) of 20 uM calmidazolium, a membrane-permeable calmodulin inhibitor. *, *t*-test P values <0.05 for recovery levels at different time points.

(Poisson) for 100-Hz trains, whereas the depression was 18.7 ± 0.4% (regular) and 30.5 ± 3.1% (Poisson, $P < 0.05$, ANOVA, post hoc test, $n = 3–6$) for 200-Hz trains (Fig. 6*B*). In contrast, the recovery time course was significantly different between regular and Poisson-like trains for 100 Hz but not for 200 Hz (Fig. 6*C*). The recovery time constants for 100-Hz stimuli were 153.8 ± 30.6 ms (regular) versus 60.9 ± 13.1 ms (Poisson, $P = 0.048$, 1-tailed *t*-test, $n = 3, 6$; *, *t*-test P values <0.05 for recovery at different time points). For 200-Hz trains, there was no difference in recovery kinetics between regular and Poisson-like spike trains. The recovery time constants were 62.5 ± 18.0 ms (regular) versus 70.4 ± 8.9 ms (Poisson, $P = 0.66$, *t*-test, $n = 3, 6$). Thus compared with regular trains, Poisson-like trains at 100 Hz promoted rapid recovery from synaptic depression, perhaps because of larger intracellular [Ca^{2+}] accumulation produced during brief bouts of high presynaptic spike rates within Poisson-like trains.

DISCUSSION

Synaptic transmission at the first central auditory synapse is a dynamic process. In mature mice (P22-38), we found that short-term synaptic depression at this synapse is primarily caused by a depletion of releasable presynaptic vesicles with little evidence for a role of postsynaptic receptor desensitization. In addition, the rate of recovery from the depression is mediated by activity-dependent mechanisms that depend on presynaptic [Ca^{2+}]. This depletion-based synaptic depression, together with its dynamically regulated recovery process, plays a key role in the functional coupling between the auditory nerve fiber and the bushy neuron.

Synaptic depression at mature endbulb synapse

We showed that synaptic depression at the endbulb from 22- to 38-day-old CBA mice does not seem to involve postsynaptic receptor desensitization. Two observations support this contention. First, using γ-DGG to minimize receptor activation and synaptic currents did not change synaptic depression or the paired-pulse ratio. Second, the paired-pulse ratio for 10 ms Δt is ~0.95 ($EPSC_2/EPSC_1$), which is much larger than expected if receptor desensitization were present at the time of the second EPSC. These observations are in contrast to a recent study in P15-21 animals (Yang and Xu-Friedman 2008), where the paired-pulse ratio at 10 ms Δt was 0.63 and where a portion of the depression appears to be mediated by postsynaptic receptor desensitization. It is likely that this represents a continued developmental shift in synaptic function as the animal matures. Our results are consistent with the developmental maturation of AMPA receptor current at the endbulb synapse (Bellingham et al. 1998). Similar observations have been made in the analogous terminals in chick (Lu and Trussell 2007) and in the MNTB calyx terminal (Joshi and Wang 2002). Thus receptor desensitization does not seem to contribute to synaptic depression in older mice at the endbulb synapse.

It is possible that a portion of the depression during repetitive synaptic activation in older animals is caused by short-term changes in Ca^{2+}-sensitive release probability during the train (von Gersdorff and Borst 2002; Wolfel et al. 2007). Compared with endbulb terminals from younger mice (Oleskevich and Walmsley 2002; Xu-Friedman and Regehr 2005b; Yang and Xu-Friedman 2008), the steady-state depression level in our mature endbulbs was generally smaller (~40 vs. 80–90% at 100 Hz). This could be explained by the amount of postsynaptic receptor desensitization observed at immature synapses (Raman and Trussell 1992; Trussell et al. 1993; Yang and Xu-Friedman 2008), the difference in initial release probability between ages (Bellingham et al. 1998; Joshi and Wang 2002), the difference in intrinsic Ca^{2+} buffering capability and in Ca^{2+} sensitivity for vesicle release (Fedchyshyn and Wang 2005; Felmy and Schneggenburger 2004; Wadel et al. 2007), and the difference in Ca^{2+}-dependent recovery (Yang and Xu-Friedman 2008).

Ca^{2+}-dependent recovery from depression

Ca^{2+} dependence of recovery from short-term synaptic depression has been reported at the endbulb terminal (Yang and Xu-Friedman 2008) as well as at various other CNS synapses (Dittman and Regehr 1998; Sakaba and Neher 2001a; Stevens and Wesseling 1999; Wang and Kaczmarek 1998). Yang and Xu-Friedman (2008) showed that the Ca^{2+}-dependent recovery is critical to counteract the effect of depletion-based synaptic depression at the endbulb synapse. They also showed that synaptic recovery from a high-frequency stimulus train recovered with fast and slow time constants of ~40 ms and ~2 s, very similar to our results. A simple model incorporating Ca^{2+}-dependent replenishment of a single releasable vesicle pool appears to catch the essence of two-phased recovery at the endbulb terminal (Yang and Xu-Friedman 2008). However, unlike the dual-recovery after a 100-Hz train reported, our data showed only a slow recovery (~2 s) at 100 Hz (Fig. 3). Moreover, even increasing the external Ca^{2+} from 1.5 to 2 mM at 100 Hz did not seem to induce a faster component (Figs. 3 and 4). This suggests that a strictly Ca^{2+}-facilitated model of a single releasable vesicle pool (Yang and Xu-Friedman 2008) may be insufficient to explain the fast recovery. It appears that the fast recovery mechanism requires intracellular Ca^{2+} accumulation to reach certain "threshold" that is achieved only at higher firing rates or perhaps by certain firing patterns. It is not clear what the intracellular Ca^{2+} "threshold" is, although

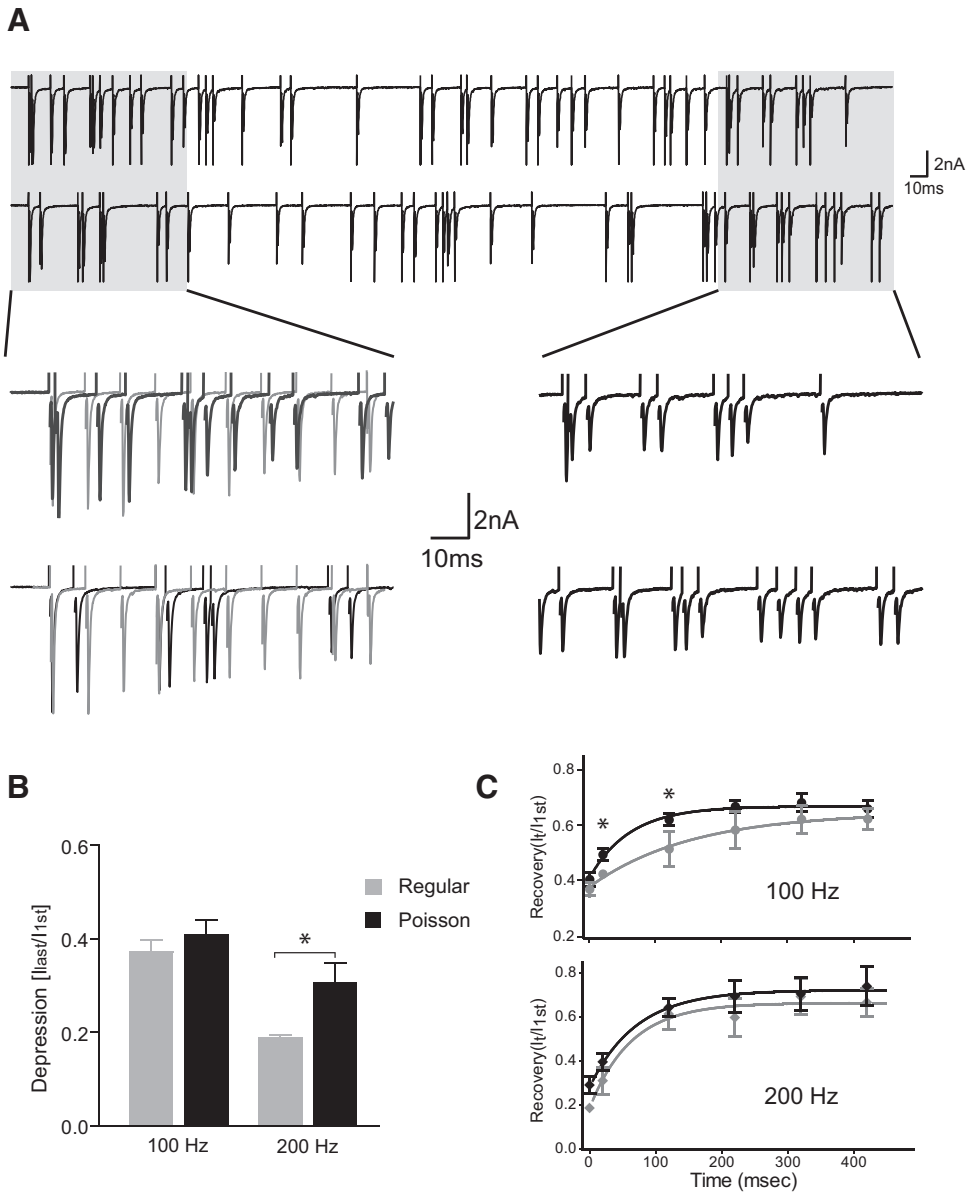

FIG. 6. Synaptic depression and recovery with 100-Hz regular and Poisson-like spike trains. *A*: sample EPSCs from 100-Hz Poisson-like spike trains. EPSCs from 100-Hz regular trains (faint traces) were superimposed in the 1st 100 ms expanded view to compare the rate of depression between 2 types of stimulus trains. *B*: the normalized mean EPSCs from both regular and Poisson-like trains at the end of 500-ms stimulation. *C*: synaptic recovery time course after the 100- and 200-Hz regular and Poisson-like trains.

studies at the calyx terminal in MNTB using a two vesicle pool model suggest it may be ~6 μM (Sakaba and Neher 2001a,b, 2003; Wadel et al. 2007; Wu and Borst 1999). We also note that the fast recovery time constant seems to be fairly similar under different intracellular Ca^{2+} conditions, e.g., 200 versus 300 Hz, suggesting that it may be governed by a process that is triggered by elevated intraterminal calcium but is not linearly related to $[Ca^{2+}]_i$. Our data appear to be more consistent with a two-vesicle-pool model, which suggests the replenishment of the slow releasing vesicles, once released under conditions of high $[Ca^{2+}]_i$, is less correlated with further internal Ca^{2+} change (Sakaba and Neher 2001a,b, 2003; Wadel et al. 2007). The involvement of a Ca^{2+}/calmodulin signaling in the fast recovery (Fig. 5) (also see Sakaba and Neher 2001a) further supports a "threshold" triggering mechanism.

Depression and recovery with Poisson-like stimulus trains

The spontaneous and some sound driven activity of auditory nerve fibers exhibit exponentially distributed interspike intervals approximating a Poisson renewal process. During such Poisson-like spike trains, brief bursts of interspike intervals that are much shorter than the mean interval will occur, along with periods of slower firing. If the high-frequency bursts of spikes drive a nonlinear process that decays slowly relative to the mean interspike interval, then the net accumulation of Ca^{2+} during a Poisson-like train and a regular train may be different. It has been estimated a single action potential in the MNTB calyx can cause intracellular Ca^{2+} to rise locally to 10 μM and then decay to resting levels within 10–20 ms (Bollmann and Sakmann 2005; Spirou et al. 2008). More mature terminals have high endogenous Ca^{2+} buffering capability (Felmy and Schneggenburger 2004) and thus may prevent significant accumulation of $[Ca^{2+}]_i$ at stimulus rates <100 Hz. We observed a faster recovery from depression after a 500-ms Poisson-like train at 100 Hz than with a regular train at the same frequency (Fig. 6*C*). Together with our other observations, this suggests that the 100-Hz Poisson-like train resulted in a higher average terminal $[Ca^{2+}]_i$ than the regularly spaced 100-Hz train. It

further suggests that the $[Ca^{2+}]_i$ decays faster in the mature endbulb terminal, perhaps due to greater Ca^{2+} buffering capacity or faster buffering kinetics. It would be interesting to experimentally verify the high-Ca^{2+} accumulation in the endbulb terminal with Poisson-like stimuli. Surprisingly, we observed smaller synaptic depression with 200 Hz but not 100-Hz Poisson trains, especially in view of the fact that recovery is faster with Poisson-distributed trains at 100 Hz. One possibility is that our Poisson-distributed trains (500 ms) were too brief to observe the "benefit" of fast recovery within the Poisson train of such short-duration, although similar experiments in MNTB calyx used trains of 2 min showed similar results to ours at lower rates (≤60 Hz) (Hermann et al. 2007). For 200-Hz trains, recovery seems to benefit from the lulls in activity, allowing more complete recovery from depression (overshot part in Figs. 3–4) within Poisson-distributed trains of even short-duration.

Functional implications of fast and slow recovery

Considering the function of bushy neurons in vivo, there is an obvious advantage to have rapid synaptic recovery during periods of high afferent firing rates. Modeling studies have suggested that the synapse will be depleted very quickly without a Ca^{2+}-facilitated replenishment mechanism (Yang and Xu-Friedman 2008). However, it is not obvious why it takes quite a few seconds for a synapse to fully recover to the rest state at lower rates. The number and SR configuration of auditory nerve fibers that converge on bushy cells have been actively discussed (Lu and Trussell 2007; Nicol and Walmsley 2002; Rothman et al. 1993; Xu-Friedman and Regehr 2005a,b). Data from MNTB calyx terminals (Hermann et al. 2007) suggest that even at 25 Hz, which is a low rate relative to sound-evoked activity in the afferent fibers, significant depression occurs. Thus most auditory nerve synapses (with the exception of those with spontaneous rate <1 Hz) are likely to operate in a chronically depressed state perhaps due to little or no terminal Ca^{2+} accumulation. Spontaneous activity appears to bias the synapses into a slightly depressed state in silence, such that further synaptic depression is reduced during periods of sound-driven activity, thus ensuring more reliable suprathreshold synaptic transmission between the auditory nerve fibers and bushy neurons (Brenowitz and Trussell 2001b; but also see Hermann et al. 2007). The spontaneous activity also appears to place the synapses into an operating regime where driven activity will trigger the mechanisms that promote rapid recovery from depression and further facilitate transmission onto the bushy cells.

ACKNOWLEDGMENTS

We thank Drs. Jaime Mancilla and Ruili Xie for critical reading of the manuscript.

GRANTS

This work was supported by National Institute of Deafness and Other Communication Disorders Grants R01DC-04551 to P. B. Manis and R03DC-008190 to Y. Wang.

REFERENCES

Bellingham MC, Lim R, Walmsley B. Developmental changes in EPSC quantal size and quantal content at a central glutamatergic synapse in rat. *J Physiol* 511: 861–869, 1998.

Bellingham MC, Walmsley B. A novel presynaptic inhibitory mechanism underlies paired pulse depression at a fast central synapse. *Neuron* 23: 159–170, 1999.

Bollmann JH, Sakmann B. Control of synaptic strength and timing by the release-site Ca^{2+} signal. *Nat Neurosci* 8: 426–434, 2005.

Bollmann JH, Sakmann B, Borst JG. Calcium sensitivity of glutamate release in a calyx-type terminal. *Science* 289: 953–957, 2000.

Brenowitz S, Trussell LO. Maturation of synaptic transmission at end-bulb synapses of the cochlear nucleus. *J Neurosci* 21: 9487–9498, 2001a.

Brenowitz S, Trussell LO. Minimizing synaptic depression by control of release probability. *J Neurosci* 21: 1857–1867, 2001b.

Caspary DM, Backoff PM, Finlayson PG, Palombi PS. Inhibitory inputs modulate discharge rate within frequency receptive fields of anteroventral cochlear nucleus neurons. *J Neurophysiol* 72: 2124–2133, 1994.

Dittman JS, Regehr WG. Contributions of calcium-dependent and calcium-independent mechanisms to presynaptic inhibition at a cerebellar synapse. *J Neurosci* 16: 1623–1633, 1996.

Dittman JS, Regehr WG. Calcium dependence and recovery kinetics of presynaptic depression at the climbing fiber to Purkinje cell synapse. *J Neurosci* 18: 6147–6162, 1998.

Fedchyshyn MJ, Wang LY. Developmental transformation of the release modality at the calyx of held synapse. *J Neurosci* 25: 4131–4140, 2005.

Felmy F, Schneggenburger R. Developmental expression of the Ca^{2+}-binding proteins calretinin and parvalbumin at the calyx of held of rats and mice. *Eur J Neurosci* 20: 1473–1482, 2004.

Forsythe ID, Tsujimoto T, Barnes-Davies M, Cuttle MF, Takahashi T. Inactivation of presynaptic calcium current contributes to synaptic depression at a fast central synapse. *Neuron* 20: 797–807, 1998.

Helmchen F, Borst JG, Sakmann B. Calcium dynamics associated with a single action potential in a CNS presynaptic terminal. *Biophys J* 72: 1458–1471, 1997.

Hermann J, Pecka M, von Gersdorff H, Grothe B, Klug A. Synaptic transmission at the calyx of Held under in vivo like activity levels. *J Neurophysiol* 98: 807–820, 2007.

Isaacson JS, Walmsley B. Amplitude and time course of spontaneous and evoked excitatory postsynaptic currents in bushy cells of the anteroventral cochlear nucleus. *J Neurophysiol* 76: 1566–1571, 1996.

Joshi I, Wang LY. Developmental profiles of glutamate receptors and synaptic transmission at a single synapse in the mouse auditory brain stem. *J Physiol* 540: 861–873, 2002.

Kachar B. Asymmetric illumination contrast: a method of image formation for video light microscopy. *Science* 227: 766–768, 1985.

Kindmark H, Kohler M, Gerwins P, Larsson O, Khan A, Wahl MA, Berggren PO. The imidazoline derivative calmidazolium inhibits voltage-gated Ca(2+)-channels and insulin release but has no effect on the phospholipase C system in insulin producing RINm5F-cells. *Biosci Rep* 14: 145–158, 1994.

Kopp-Scheinpflug C, Dehmel S, Dorrscheidt GJ, Rubsamen R. Interaction of excitation and inhibition in anteroventral cochlear nucleus neurons that receive large endbulb synaptic endings. *J Neurosci* 22: 11004–11018, 2002.

Kopp-Scheinpflug C, Fuchs K, Lippe WR, Tempel BL, Rubsamen R. Decreased temporal precision of auditory signaling in Kcna1-null mice: an electrophysiological study in vivo. *J Neurosci* 23: 9199–9207, 2003.

Leao RM, Kushmerick C, Pinaud R, Renden R, Li GL, Taschenberger H, Spirou G, Levinson SR, von Gersdorff H. Presynaptic Na^+ channels: locus, development, and recovery from inactivation at a high-fidelity synapse. *J Neurosci* 25: 3724–3738, 2005.

Li J, Young ED. Discharge-rate dependence of refractory behavior of cat auditory-nerve fibers. *Hear Res* 69: 151–162, 1993.

Liberman MC. Auditory-nerve response from cats raised in a low-noise chamber. *J Acoust Soc Am* 63: 442–455, 1978.

Liberman MC. Central projections of auditory-nerve fibers of differing spontaneous rate. I. Anteroventral cochlear nucleus. *J Comp Neurol* 313: 240–258, 1991.

Lu T, Trussell LO. Development and elimination of endbulb synapses in the chick cochlear nucleus. *J Neurosci* 27: 808–817, 2007.

Manis PB. Biophysical specialization of neurons that encode timing. In: *The Senses, A Comphensive Reference*, edited by Basbaum AI, Kaneko A, Shepherd GM, Wesseling JF. San Diego, CA: Academic, 2008, p. 565–586.

Nakazawa K, Higo K, Abe K, Tanaka Y, Saito H, Matsuki N. Blockade by calmodulin inhibitors of Ca^{2+} channels in smooth muscle from rat vas deferens. *Br J Pharmacol* 109: 137–141, 1993.

Nicol MJ, Walmsley B. Ultrastructural basis of synaptic transmission between endbulbs of Held and bushy cells in the rat cochlear nucleus. *J Physiol* 539: 713–723, 2002.

Ohlemiller KK, Echteler SM, Siegel JH. Factors that influence rate-versus-intensity relations in single cochlear nerve fibers of the gerbil. *J Acoust Soc Am* 90: 274–287, 1991.

Oleskevich S, Clements J, Walmsley B. Release probability modulates short-term plasticity at a rat giant terminal. *J Physiol* 524: 513–523, 2000.

Oleskevich S, Walmsley B. Synaptic transmission in the auditory brainstem of normal and congenitally deaf mice. *J Physiol* 540: 447–455, 2002.

Oleskevich S, Youssoufian M, Walmsley B. Presynaptic plasticity at two giant auditory synapses in normal and deaf mice. *J Physiol* 560: 709–719, 2004.

Otis T, Zhang S, Trussell LO. Direct measurement of AMPA receptor desensitization induced by glutamatergic synaptic transmission. *J Neurosci* 16: 7496–7504, 1996.

Pfeiffer RR. Anteroventral cochlear nucleus: wave forms of extracellularly recorded spike potentials. *Science* 154: 667–668, 1966.

Raman IM, Trussell LO. The kinetics of the response to glutamate and kainate in neurons of the avian cochlear nucleus. *Neuron* 9: 173–186, 1992.

Renden R, Taschenberger H, Puente N, Rusakov DA, Duvoisin R, Wang LY, Lehre KP, von Gersdorff H. Glutamate transporter studies reveal the pruning of metabotropic glutamate receptors and absence of AMPA receptor desensitization at mature calyx of held synapses. *J Neurosci* 25: 8482–8497, 2005.

Rodieck RW, Kiang NY, Gerstein GL. Some quantitative methods for the study of spontaneous activity of single neurons. *Biophys J* 2: 351–368, 1962.

Rothman JS, Young ED, Manis PB. Convergence of auditory nerve fibers onto bushy cells in the ventral cochlear nucleus: implications of a computational model. *J Neurophysiol* 70: 2562–2583, 1993.

Ryugo DK, Parks TN. Primary innervation of the avian and mammalian cochlear nucleus. *Brain Res Bull* 60: 435–456, 2003.

Sachs MB, Abbas PJ. Rate versus level functions for auditory-nerve fibers in cats: tone-burst stimuli. *J Acoust Soc America* 56: 1835–1847, 1974.

Sakaba T, Neher E. Calmodulin mediates rapid recruitment of fast-releasing synaptic vesicles at a calyx-type synapse. *Neuron* 32: 1119–1131, 2001a.

Sakaba T, Neher E. Preferential potentiation of fast-releasing synaptic vesicles by cAMP at the calyx of Held. *Proc Natl Acad Sci USA* 98: 331–336, 2001b.

Sakaba T, Neher E. Direct modulation of synaptic vesicle priming by GABA(B) receptor activation at a glutamatergic synapse. *Nature* 424: 775–778, 2003.

Schneggenburger R, Neher E. Intracellular calcium dependence of transmitter release rates at a fast central synapse. *Nature* 406: 889–893, 2000.

Spirou GA, Chirila FV, von Gersdorff H, Manis PB. Heterogeneous Ca(2+) influx along the adult calyx of held: a structural and computational study. *Neuroscience* 154: 171–185, 2008.

Stevens CF, Wesseling JF. Identification of a novel process limiting the rate of synaptic vesicle cycling at hippocampal synapses. *Neuron* 24: 1017–1028, 1999.

Taberner AM, Liberman MC. Response properties of single auditory nerve fibers in the mouse. *J Neurophysiol* 93: 557–569, 2005.

Trussell LO. Central synapses that preserve auditory timing. In: *The Senses: A Comprehensive Reference*, edited by Basbaum AI, Kaneko A, Shepherd GM, Westheimer G. San Diego, CA: Academic, 2008, p. 587–602.

Trussell LO, Zhang S, Raman IM. Desensitization of AMPA receptors upon multiquantal neurotransmitter release. *Neuron* 10: 1185–1196, 1993.

Turecek R, Trussell LO. Presynaptic glycine receptors enhance transmitter release at a mammalian central synapse. *Nature* 411: 587–590, 2001.

von Gersdorff H, Borst JG. Short-term plasticity at the calyx of held. *Nat Rev Neurosci* 3: 53–64, 2002.

Wadel K, Neher E, Sakaba T. The coupling between synaptic vesicles and Ca(2+) channels determines fast neurotransmitter release. *Neuron* 53: 563–575, 2007.

Wang LY, Kaczmarek LK. High-frequency firing helps replenish the readily releasable pool of synaptic vesicles. *Nature* 394: 384–388, 1998.

Wang Y, Manis PB. Synaptic transmission at the cochlear nucleus endbulb synapse during age-related hearing loss in mice. *J Neurophysiol* 94: 1814–1824, 2005.

Wang Y, Manis PB. Temporal coding by cochlear nucleus bushy cells in DBA/2J mice with early onset hearing loss. *J Assoc Res Otolaryngol* 7: 412–424, 2006.

Wickesberg RE, Oertel D. Tonotopic projection from the dorsal to the anteroventral cochlear nucleus of mice. *J Comp Neurol* 268: 389–399, 1988.

Winter IM, Robertson D, Yates GK. Diversity of characteristic frequency rate-intensity functions in guinea pig auditory nerve fibers. *Hear Res* 45: 191–202, 1990.

Wolfel M, Lou X, Schneggenburger R. A mechanism intrinsic to the vesicle fusion machinery determines fast and slow transmitter release at a large CNS synapse. *J Neurosci* 27: 3198–3210, 2007.

Wong AY, Graham BP, Billups B, Forsythe ID. Distinguishing between presynaptic and postsynaptic mechanisms of short-term depression during action potential trains. *J Neurosci* 23: 4868–4877, 2003.

Wu LG, Borst JG. The reduced release probability of releasable vesicles during recovery from short-term synaptic depression. *Neuron* 23: 821–832, 1999.

Xu J, Wu LG. The decrease in the presynaptic calcium current is a major cause of short-term depression at a calyx-type synapse. *Neuron* 46: 633–645, 2005.

Xu-Friedman MA, Regehr WG. Dynamic-clamp analysis of the effects of convergence on spike timing. I. Many synaptic inputs. *J Neurophysiol* 94: 2512–2525, 2005a.

Xu-Friedman MA, Regehr WG. Dynamic-clamp analysis of the effects of convergence on spike timing. II. Few synaptic inputs. *J Neurophysiol* 94: 2526–2534, 2005b.

Yang H, Xu-Friedman MA. Relative roles of different mechanisms of depression at the mouse endbulb of Held. *J Neurophysiol* 99: 2510–2521, 2008.

Zhang S, Trussell LO. A characterization of excitatory postsynaptic potentials in the avian nucleus magnocellularis. *J Neurophysiol* 72: 705–718, 1994.

Zucker RS, Regehr WG. Short-term synaptic plasticity. *Annu Rev Physiol* 64: 355–405, 2002.